Designing and studying of PVA/Fe_2O_3/Se as new ovonic material for possible storage application

K. A. Mohammed[ab*], K. H. Salem[c], M. F. Jawaad[d], M. A. Alkhafaji[e], R. S. Zabibah[f]
[a]*Faculty of Pharmacy, Jabir Ibn Hayyan Medical University, Kufa, Iraq*
[b]*Department of medical physics, Hilla University College, Babylon, Iraq*
[c]*College of Medical and Health Technologies, Al-Zahraa University for Women, Karbala, Iraq.*
[d]*Department of physics, College of science, University of kerbala, Kerbala, Iraq*
[e]*National University of Science and Technology, Dhi qar, Iraq*
[f]*Medical Laboratory Technology Department, College of Medical Technology, The Islamic University, Najaf, Iraq.*

This study presents the synthesis of a novel ovonic nanomaterial by the chemical route approach, involving the combination of three distinct materials: polyvinyl alcohol (PVA), iron oxide (Fe2O3), and selenium (Se) nanoparticles. The produced material underwent evaluation using various analytical techniques, including Xray diffraction (XRD), energy-dispersive Xray spectroscopy (EDS), scaning electron microscope (SEM), and UV-Visible spectrophotometer. The focus of the work revolved around a unique hybrid structure consisting of selenium nanoparticles that were embedded within a polyvinyl alcohol and iron(III) oxide. The examination of micro structure information yielded findings that support the notion that Se nanoparticles have an impact on the structural properties of PVA/Fe_2O3. (XRD) and (EDS) examines provided confirmation of the formation of a novel composite structure. The produced composites had notable absorption peaks at a wavelength of 530 nm for PVA-Fe_2O_3-CdZnS. These composites exhibited a progressive transition towards absorption in higher wavelength areas. The composite material that has been suggested for potential utilization in forthcoming energy storage applications.

(Received August 24, 2023; Accepted November 1, 2023)

Keywords: Iron oxide, Polymer matrix, Selenium nanoparticles, Ovonic nanomaterials

1. Introduction

Magnetic nanoparticles (MNPs), which are materials at the nanoscale, possess distinctive magnetic characteristics and have found extensive utilization across several domains including healthcare, energy, engineering, and environmental applications. In current years, there had been a important increasing in research focused on MNPs due to their exceptional and distinctive features. These qualities have led to the exploration of their possible application in several arenas for example medicine, catalysis, agricultures, and energy storages [1-5]. Transition metals ions such as iron, cobalt, nickel, and their corresponding complexes are commonly employed in the synthesis of magnetic nanoparticles (NPs) [6-8]. Iron is an element that can exist in several forms with valences ranging from zero to three. Furthermore, many iron compounds exhibit distinct properties, ranging from magnetism to ferromagnetism [9]. The magnetic nanoparticles (NPs) encompass several iron oxides , namely Magnetite (Fe_3O4), Maghemite (γ-Fe_2O_3), Hematite (α-Fe_2O_3), and Goethite (FeO(OH)) [10,11]. Hematite demonstrates a higher thermodynamic stability compared to other iron oxides when exposed to oxygen. It also displays pronounced electron-electron interactions and electron-photon resonances, which are followed by intricate electronic structures that possess intriguing optoelectronic properties [12-14].

* Corresponding author: kahtan.a.mohammed@jmu.edu.iq
https://doi.org/10.15251/JOR.2023.196.615

Iron oxide nanoparticles (IONPs) are commonly manufactured by several processes, with physical and chemical approaches being the most prevalent. The manufacture of (IONPs) necessitates the use of potent chemical reducing agents, which can have a significant environmental impact. Therefore, it is imperative to seek a dependable, operative, and ecologically friendly approach for the fabrication of nanoparticles. The selected approach should adhere to principles of economic viability, environmental sustainability, and cost-effectiveness. Moreover, the consideration of raw material availability and natural resource accessibility is of paramount significance while selecting a methodology [15]. The compound α-Fe_2O_3, which possesses an in direct energy gap of 2.20 eV, had been recognized as a semi conductor of the n-type and finds extensive utility in several fields including catalysis, gas sensing, and photovoltaics. An optimal semiconductor possesses a substantial bandgap that can be stimulated by visible light, rendering it both environmentally and economically viable for the efficient production of large-scale field applications [16].

The growing interest in generation of energy from nonfossil energy bases, such as wind, water and solar, can be attributed to the adverse environmental impacts associated with energy derived from fossil fuels, which include global pollution and climate change. Rechargeable batteries are often regarded as the optimal energy storing technology for the purpose of stowage energy derived from renewable bases, owing to their substantial storage capacity and exceptional conversion efficiency. [17] Iron oxide-based anodes are very promising options for energy storage systems such as lithium-ion batteries due to their advantageous properties, including abundance, low cost, and non-toxicity [18]. Se, an element that belongs to the similar group as sulfur in the periodic table and demonstrates a comparable redox process, has been suggested as a prospective cathode material for rechargeables lithium based batteries. This phenomenon can be attributed to the several advantages it presents in comparison to widely researched sulfur systems [19].

Selenium (Se), a semiconductor of interest in the field of chalcogenides, has historically been employed for the purpose of harnessing solar energy. The advancement of nanoscience and nanotechnology has facilitated the creation of a wide range of selenium (Se) nanoparticles that possess intricate architectures and distinctive characteristics. Upon comparison with other chalcogens, it becomes evident that selenium nanoparticles possess an anisotropic crystalline structure, intrinsic chirality, and exhibit a notable level of reactivity. Moreover, these materials exhibit exceptional physicochemical properties. The incorporation of selenium (Se) nanoparticles into materials of technical importance, such as conductors and semiconductors, on substrate that is plastic, bendy, stretchable, and extremely curved, represents a significant and advanced development in the realm of flexible and wearable electronics utilizing Se nanomaterials [20]. Recent research has also indicated the significant potential of selenium nanoparticles in serving as great performances electrode for energy storing device. Lithium-sulfur battery commonly exhibit notable theoretic definite capacity for energy. Nevertheless, the implementation of these methods has been impeded by two significant challenges. Sulfur is not considered an optimal choice for an electrode material due to its inherent limitations in terms of both electronic and ionic conductivity. Furthermore, during battery operation, electrolyte-soluble poly sulfide inter mediate products exhibit solubility in fluid electrolyte, resulting in the notable shuttle effect and subsequent capacity degradation. Selenium (Se) has emerged as a viable substitute for sulfur in the context of electrodes material for lithium-selenium (Li-Se) battery [21-25].

In this work, a simple and one-step chemical method was applied to prepare PVA/ Fe_2O_3/Se nanocomposite. The PVA/ Fe_2O_3/Se nanocomposites were tested by some instruments to study their optical and structural properties.

2. Materials Used and methods

2.1. Synthesis of PVA/ Fe_2O_3/Se nanocomposite materials

For purpose of facilitate the synthesis of PVA/ Fe_2O_3/Se, a colloid comprising the iron precursor had been made by mixing 50 milliliters (ml) of de ionized water with one gram of ferric chloride ($FeCl_3$). A complex agent, consisting of a solvent comprising 1% polyvinyl alcohol, had been utilized in the experiment. A composite was created by blending 10 mL of (PVA) with 10

mL of (FeCl3) containing 0.1 g of selenium (Se) nanoparticles. Following that, a minute volume of 1 milliliter of a 1 molar solution of sodium hydroxide (NaOH) was introduced into the resultant combination. Following that, the solutions underwent a thermal treatment at a temp. equal to 70 C^o and were stirred for a period of one hour utilizing a hot plate. The examination and publication of the PVA/ Fe_2O_3 nanoparticles without Se were conducted and documented in this scholarly work [26]. Table 1 shows the prepared samples.

Table 1. displays the information of prepared samples.

sample	Information
Se 0	PVA/ Fe_2O_3
Se 1	PVA/ Fe_2O_3/Se

3. Results and discussion

Fig. 1 presentations the FESEM pictures of the PVA/ Fe_2O_3/Se nanocomposite prepared by the chemical route. In figure 1 two magnification zones of PVA/ $Fe_2O_3$3/Se were presented, they contain agglomeration area from polymer surrounding the particles. There is no ability to identify the different particles where all type of particles mixed well together.

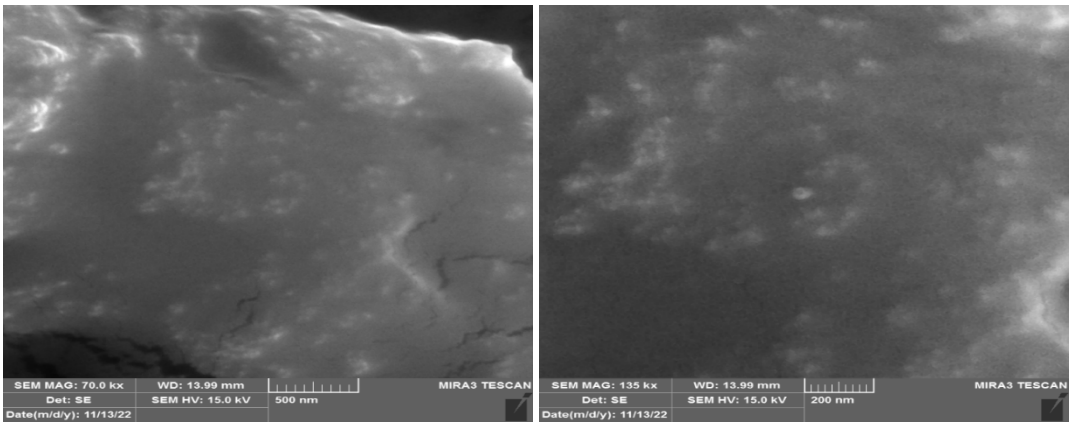

Fig. 1. Represents the morphology of (Se 1) composite material by SEM.

The presence of elemental selenium (Se), carbon (C), iron (Fe), and oxygen (O) in the synthesized nanocomposite had been scanned by (EDS). Fig. 5 displays the spectra of the PVA/ Fe_2O_3/Se nanocomposite. The presence of prominent peaks at around 1.8 keV and 6.2 keV indicates that the principal constituents of the sample are the elements selenium (Se) and iron (Fe). The weight percent composition of carbon and iron was determined to be 48% and 45%, respectively, while oxygen accounted for the remaining percentage. The remaining proportion is attributed to the elements Fe and Se.

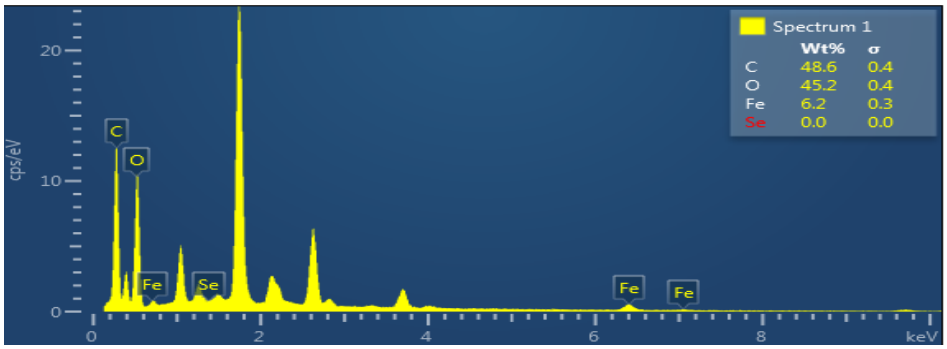

Fig. 2. EDS spectrum of Se 1 composite.

XRD data collected had been ready for identifying the nanocomposite construction. Figure 3 shows the peak of composite and the inset figure represent the Fe_2O_3 peak . As was cleared in inset Figure 1, for Fe_2O_3 the recognized strong peak at 32° and 58.5° were given to the crystallographics information of the α- Fe_2O_3 phases [16]. Peak at 18,28 belonging to FeSe combination according to ref. [27] peak at 21, 26, 35, 43 belonging to Se according to ref. [28]. Table 2. Shows the information about structural properties of Se 1 sample.

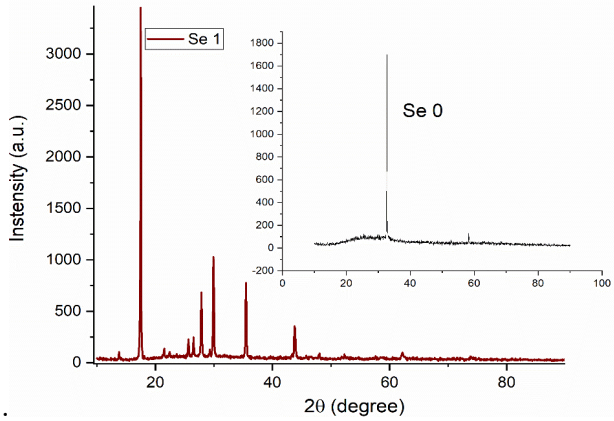

Fig. 3. XRD peaks position of Se 1 sample.

Table 2. Shows the information about structural properties of Se 1 sample.

Position [°θ]	Intensity[a. u.]	FWHM [°2θ.]	d-space [Å]	Rael. Intensity [%]	Tip Width
17.5000	3393(52)	0.123(2)	5.06365	100.00	0.1475
21.4	83(11)	0.18(5)	4.13359	2.43	0.2142
22.42	58(9)	0.19(5)	3.96308	1.70	0.2281
25.644	166(14)	0.17(3)	3.47096	4.90	0.2096
26.515	193(17)	0.14(2)	3.35889	5.68	0.1725
27.856	652(22)	0.182(9)	3.20025	19.22	0.2189
29.924	1041(27)	0.168(5)	2.98362	30.67	0.2019
35.476	737(21)	0.174(6)	2.52833	21.71	0.2086
41.37	12(6)	0.2(1)	2.18077	0.35	0.2368
43.813	315(12)	0.26(1)	2.06462	9.29	0.3060
47.98	42(6)	0.24(4)	1.89443	1.25	0.2871
52.3	10(3)	1.0(3)	1.74697	0.30	1.1759
62.21	53(5)	0.44(5)	1.49100	1.56	0.5302
74.02	21(3)	0.6(1)	1.27970	0.61	0.7503

The transmission of prepared composite was displayed in figure 4. From the figure and comparing the inset spectrum which is belong to PVA/ Fe_2O_3 the transmission range of PVA/ Fe_2O_3 approximate to the PVA/ Fe_2O_3 both martials have high transmission for visible wavelengths above 550 nm and small transmission in the region 550 nm and less

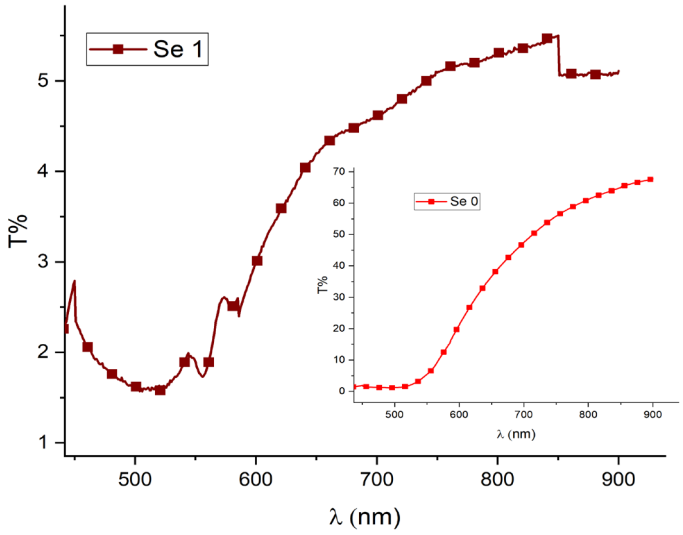

Fig. 4. Spectra of transmission of prepared samples.

In Figure 5, the absorbance spectrum of the Se 0 and spectrum Se1 materials are displayed, revealing peak absorptions at wavelengths of 500 nm and 530 nm for the Se 0 and Se 1 samples, respectivly. It is worth noting that the absorption min. of the Se 1 composite exhibits a gradual shift towards higher wavelengths. It could be prominent that the absorption of the Se 1 progressively shifted toward higher wavelengths. Absorption coefficient of prepared samples are presented in figure 6.

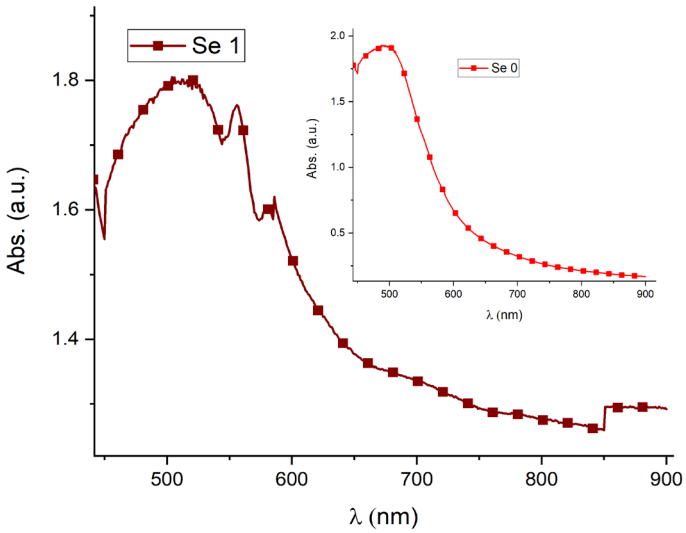

Fig. 5. Spectra of absorbance for prepared samples.

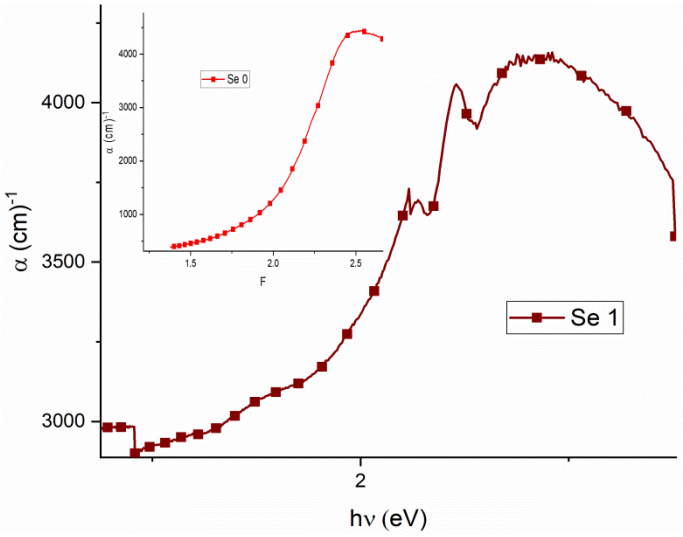

Fig. 6. Absorption coefficients of prepared samples.

The calculated values for the indirect gap energy between the conduction and valence bands in samples Se 0 and Se 1 are 2.3 eV and 1.94 eV, respectively, as determined from the Tauc plot shown in Figure 7. While fig. 8 displays the direct band gaps of Se 0 and Se 1 are 2.2 eV and 2 eV respectively [29,30].

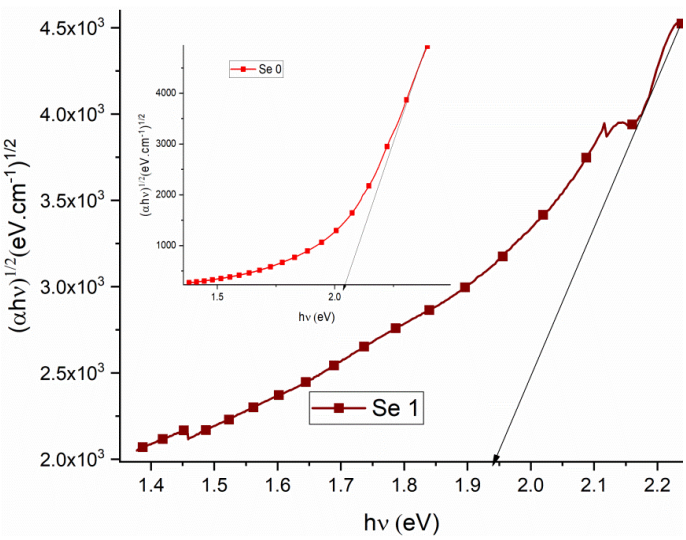

Fig. 7. Indirect band gap of Se 0 and Se 1 composites.

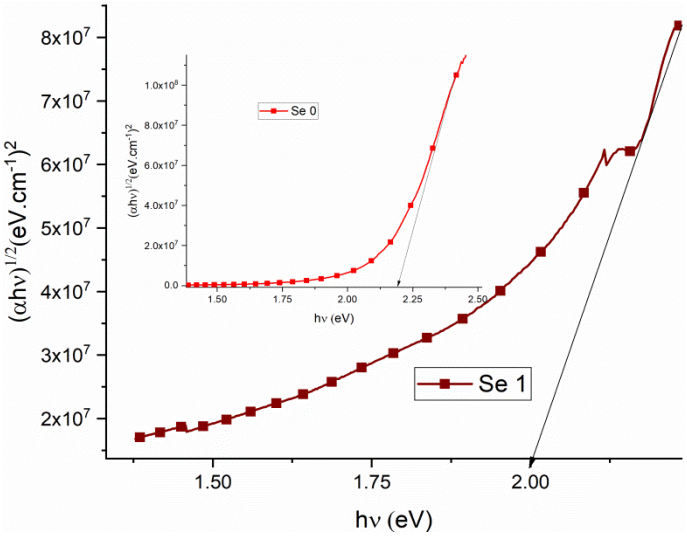

Fig. 8. Direct band gap of Se 0 and Se 1 composites.

4. Conclusions

In this study, a novel PVA/Fe_2O_3/Se nanocomposites were successfully synthesized by chemical synthesis method. The synthesis of PVA/ Fe_2O_3/Se composites were confirmed by various characterizing techniques. The examination of microstructure data yielded findings that support the notion that Se nanoparticles have an impact on the structural properties of PVA/Fe_2O_3.

The (XRD) and (EDS) analyses provided confirmation of the formation of a novel composite structure. The produced composites had notable absorption peaks at a wavelength of 530 nm for PVA-Fe_2O_3-CdZnS. These composites exhibited a progressive transition towards absorption in higher wavelength areas. The composite material that has been suggested for potential utilization in forthcoming energy storage applications.

References

[1] Ali, A., Shah, T., Ullah, R., Zhou, P., Guo, M., Ovais, M., Rui, Y. (2021), Frontiers in Chemistry, 9, 629054; https://doi.org/10.3389/fchem.2021.629054

[2] Arun, T., Dhanabalan, S. S., Udayabhaskar, R., Ravichandran, K., Akbari-Fakhrabadi, A., Morel, M. J. (2022), Inorganic Materials for Energy, Medicine and Environmental Remediation, 131-150; https://doi.org/10.1007/978-3-030-79899-4_6

[3] Kianfar, E. (2021), Journal of Superconductivity and Novel Magnetism, 34(7), 1709-1735; https://doi.org/10.1007/s10948-021-05932-9

[4] Nosrati, H., Salehiabar, M., Fridoni, M., Abdollahifar, M. A., Kheiri Manjili, H., Davaran, S., & Danafar, H. (2019), Scientific reports, 9(1), 7173; https://doi.org/10.1038/s41598-019-43650-4

[5] Frey, N. A., Peng, S., Cheng, K., & Sun, S. (2009), Chemical Society Reviews, 38(9), 2532-2542; https://doi.org/10.1039/b815548h

[6] Rudakov, G. A., Tsiberkin, K. B., Ponomarev, R. S., Henner, V. K., Ziolkowska, D. A., Jasinski, J. B., Sumanasekera, G. (2019), Journal of Magnetism and Magnetic Materials, 472, 34-39; https://doi.org/10.1016/j.jmmm.2018.10.016

[7] Munir, T., Mahmood, A., Rasul, A., Imran, M., Fakhar-e-Alam, M. (2023), Materials Chemistry and Physics, 301, 127677; https://doi.org/10.1016/j.matchemphys.2023.127677

[8] Cross, S. N., Fataftah, M., Jonderian, A., McCalla, E., Blum, A. S. (2023), Journal of Magnetism and Magnetic Materials, 567, 170345; https://doi.org/10.1016/j.jmmm.2022.170345

[9] Al-Hakkani, M. F., Gouda, G. A., & Hassan, S. H. (2021), Heliyon, 7(1); https://doi.org/10.1016/j.heliyon.2020.e05806

[10] Al-Thuwaynee, A. (2019). Combustion Synthesis of Ferric Oxide (Fe_2O_3) Nanoparticles (Doctoral dissertation, University of Brighton).

[11] Yathindranath, V. (2014). Syntheses of iron oxide and other transition metal oxide nanoparticles, and their modifications for biomedical applications.

[12] Tahir, M., Fakhar-e-Alam, M., Atif, M., Mustafa, G., & Ali, Z. (2023), Journal of King Saud University-Science, 35(5), 102695; https://doi.org/10.1016/j.jksus.2023.102695

[13] Narayanan, K. B., & Han, S. S. (2016), Journal of Cluster Science, 27, 1763-1775; https://doi.org/10.1007/s10876-016-1040-9

[14] Chen, Y. H., Lin, C. C. (2014), Physics and Chemistry of Minerals, 41, 727-736; https://doi.org/10.1007/s00269-014-0686-9

[15] Sridevi, H., Bhat, M. R., Kumar, P. S., Kumar, N. M., Selvaraj, R. (2023), Applied Nanoscience, 1-9; https://doi.org/10.1007/s13204-023-02780-y

[16] Khoshnam, M., Farahbakhsh, J., Zargar, M., Mohammad, A. W., Benamor, A., Ang, W. L., & Mahmoudi, E. (2021), Scientific reports, 11(1), 20378; https://doi.org/10.1038/s41598-021-99849-x

[17] Khan, M., Ding, X., Zhao, H., Wang, Y., Zhang, N., Chen, X., Xu, J. (2022), Electrochem, 3(2), 285-308; https://doi.org/10.3390/electrochem3020020

[18] Lv, L., Peng, M., Wu, L., Dong, Y., You, G., Duan, Y., Liu, X. (2021), Progress in iron oxides based nanostructures for applications in energy storage. Nanoscale Research Letters, 16(1), 138; https://doi.org/10.1186/s11671-021-03594-z

[19] Zhang, J., Xu, Y., Fan, L., Zhu, Y., Liang, J., Qian, Y. (2015), Nano Energy, 13, 592-600; https://doi.org/10.1016/j.nanoen.2015.03.028

[20] Dang, C., Liu, M., Lin, Z., Yan, W., Chem Synth 2023;3:14; https://doi.org/10.20517/cs.2022.33

[21]Ji L, Rao M, Zheng H, et al., J Am Chem Soc 2011;133:18522-5; https://doi.org/10.1021/ja206955k

[22]Bruce PG, Freunberger SA, Hardwick LJ, Tarascon JM., Nat Mater 2011;11:19-29; https://doi.org/10.1038/nmat3191

[23]Luo C, Xu Y, Zhu Y, et al., ACS Nano 2013;7:8003-10; https://doi.org/10.1021/nn403108w

[24]Guo J, Xu Y, Wang C., Nano Lett 2011;11:4288-94; https://doi.org/10.1021/nl202297p

[25] Abouimrane A, Dambournet D, Chapman KW, Chupas PJ, Weng W, Amine K., J Am Chem Soc 2012;134:4505-8; https://doi.org/10.1021/ja211766q

[26] K. A. Mohammed , N. H. J. Al Hasan, L. R. Al-Ameer, D. S. Abdul-Zahra, Y. D. Dwivedi, K. H. Salem, M. K. Agarwal, R. S. Zabibah, M. A. Alkhafaji, Chalcogenide Letters. Vol. 20, No. 8, August 2023, p.599-608; https://doi.org/10.15251/CL.2023.208.599

[27] Xue, M. Z., & Fu, Z. W. (2007), Acta Chimica Sinica, 65(23), 2715.

[28] Prasanth, S., & Sudarsanakumar, C. (2017), New Journal of Chemistry, 41(17), 9521-9530; https://doi.org/10.1039/C7NJ00477J

[29] Kulkarni, S., Jadhav, M., Raikar, P., Barretto, D. A., Vootla, S. K., & Raikar, U. S. (2017), New Journal of Chemistry, 41(17), 9513-9520; https://doi.org/10.1039/C7NJ01849E

[30] Saranya, A., Thamer, A., Ramar, K., Priyadharsan, A., Raj, V., Murugan, K., Maheshwaran, P. (2020), Journal of Photochemistry and Photobiology B: Biology, 207, 111885; https://doi.org/10.1016/j.jphotobiol.2020.111885